

# GROMOS 53A6<sub>GLYC</sub>, an Improved GROMOS Force Field for Hexopyranose-Based Carbohydrates

Laercio Pol-Fachin,<sup>†</sup> Victor H. Rusu,<sup>‡</sup> Hugo Verli,<sup>\*,†,§</sup> and Roberto D. Lins<sup>\*,‡</sup>

<sup>†</sup>Center of Biotechnology, Federal University of Rio Grande do Sul, Porto Alegre, RS, Brazil

<sup>‡</sup>Department of Fundamental Chemistry, Federal University of Pernambuco, Recife, PE, Brazil

<sup>§</sup>College of Pharmacy, Federal University of Rio Grande do Sul, Porto Alegre, RS, Brazil

**ABSTRACT:** An improved parameter set for explicit-solvent simulations of carbohydrates (referred to as GROMOS 53A6<sub>GLYC</sub>) is presented, allowing proper description of the most stable conformation of all 16 possible aldohexopyranose-based monosaccharides. This set includes refinement of torsional potential parameters associated with the determination of hexopyranose rings conformation by fitting to their corresponding quantum-mechanical profiles. Other parameters, as the rules for third and excluded neighbors, are taken directly from the GROMOS 53A6 force field. Comparisons of the herein presented parameter set to our previous version (GROMOS 45A4), the GLYCAM06 force field, and available NMR data are presented in terms of ring puckering free energies, conformational distribution of the hydroxymethyl group, and glycosidic linkage geometries for 16 selected monosaccharides and eight disaccharides. The proposed parameter modifications have shown a significant improvement for the above-mentioned quantities over the two tested force fields, while retaining full compatibility with the GROMOS 53A6 and 54A7 parameter sets for other classes of biomolecules.

## INTRODUCTION

In recent years, glycobiology has become a critical facet of postgenomic science,<sup>1</sup> as carbohydrates have been associated with several biological events, from participating in large spatial or temporal scale processes, such as immune defense and cellular growth,<sup>2,3</sup> to influencing minor but complex properties of biomolecules, such as those related to protein glycosylation.<sup>4</sup> Such a broad range of functions achieved by carbohydrates is possibly related to their great structural diversity. In contrast to most nucleic acids and proteins, which are linear and have a unique type of linkage, glycans can be branched, linked through one of two anomeric configurations<sup>5</sup> through different atoms of their monomeric units, monosaccharides. Proper understanding of carbohydrate roles over biological systems requires an appropriate characterization, at the atomic level, of their conformation and dynamics conveyed by means of experimental and/or theoretical techniques.

Among the experimental methods, X-ray crystallography usually provides the most complete description of a structure, once a crystal is obtained for the system under study.<sup>5</sup> However, due to the flexible nature of oligosaccharides, together with the lack of strong lipophilic or dipolar inter-residue interactions and their high degree of coordination to water molecules,<sup>6</sup> carbohydrates are usually resistant to crystallization. Alternatively, NMR spectroscopy, based on the nuclear Overhauser effect (NOE), is frequently employed for obtaining or validating carbohydrate conformational profiles.<sup>7–9</sup> A caveat is that atomic coordinates are not provided, but a set of solution-averaged spatial constraints that restrict the number of possible conformations is.<sup>5</sup> In addition, NMR usually supplies a low number of NOE signals for carbohydrates,<sup>6</sup> which causes difficulties for completely determining glycan conformations. Other indirect experimental techniques, such as electron microscopy, light/neutron diffraction, or circular

dichroism, have also been used to provide useful information about carbohydrates' three-dimensional organization.<sup>10</sup>

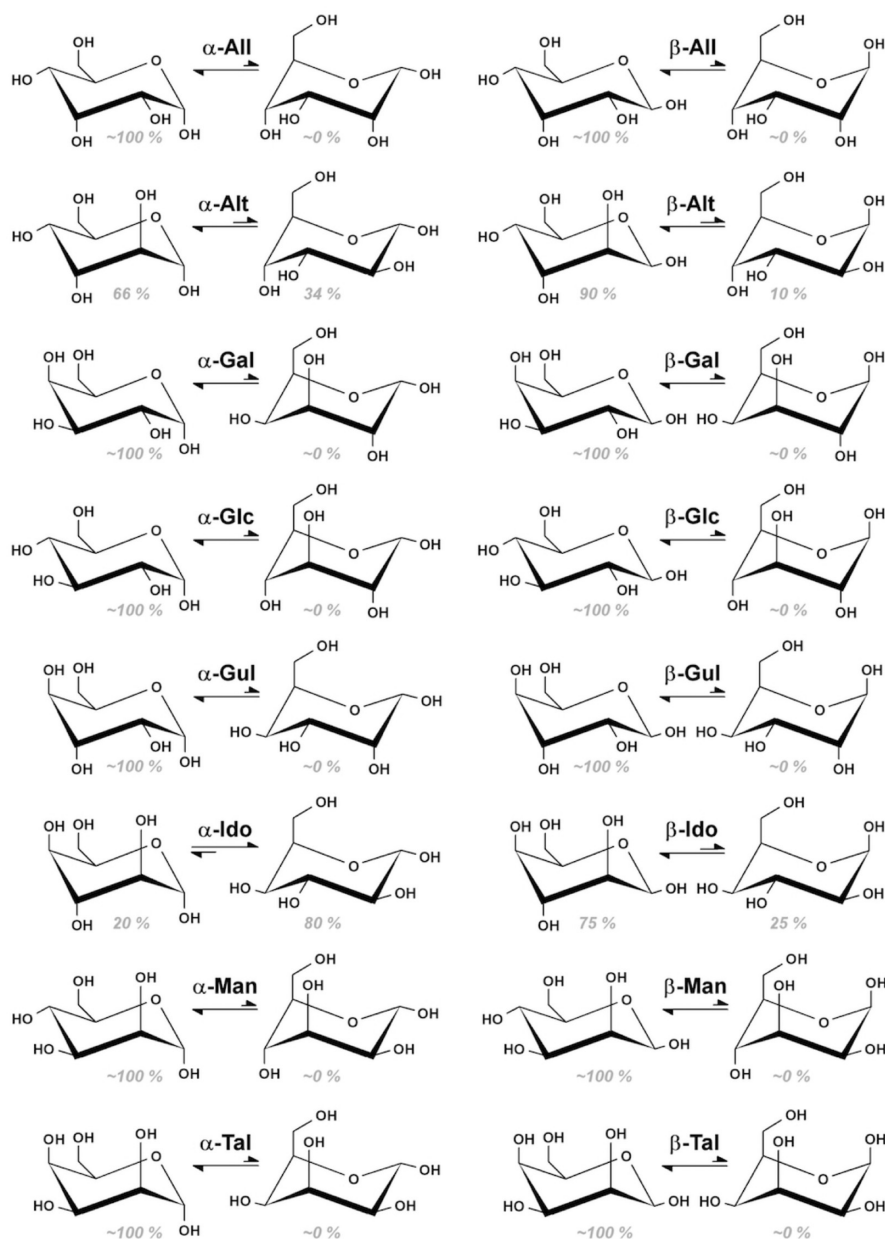
In this scenario, atomistic molecular dynamics (MD) simulations emerge as a powerful tool, providing data about carbohydrates typically inaccessible to experimental methods, with both atomic and temporal resolution.<sup>5,6,11,12</sup> The accuracy of such simulations is determined by the underlying computational model, including the accessible system size and time scale, the employed methodology, and parameters set.<sup>12</sup> In the context of the last property, among the parameter sets available for carbohydrates simulations in explicit solvent, some of the most used are included within the AMBER-GLYCAM,<sup>13,14</sup> CHARMM,<sup>15–18</sup> OPLS,<sup>19,20</sup> and GROMOS<sup>21–23</sup> force fields. Of interest to the present work, the GROMOS 45A4/53A6 force field for carbohydrates<sup>21,24</sup> has been shown to accurately describe a wide variety of polysaccharide properties<sup>25–30</sup> such as conformation,<sup>28,29</sup> dynamics,<sup>25</sup> and function.<sup>27,30</sup> However, it has been suggested that such parameters may present difficulties in reproducing internal ring puckering of a few residues and, to a lesser extent, the most stable form of specific aldohexopyranose monosaccharides.<sup>31</sup> On the basis of this information, modifications have been proposed by tuning torsional potentials by trial and error. However, a proper description of ring conformer populations was not achieved for some aldohexopyranoses.<sup>31,32</sup> Additionally, a reparameterized force field has been also suggested,<sup>12</sup> adequately describing aldohexopyranose preferred puckering conformations. The latter requires extensive modifications upon the existing parameters, i.e., new charges and atom types, several new torsional potentials, and nonstandard van der Waals scalings.<sup>12</sup>

Received: June 10, 2012

Published: September 6, 2012



Chart 1. Chemical Structures of the 16 Aldohexopyranoses Considered in the Present Study, in Their  $^4C_1$  (left) and  $^1C_4$  (right) Forms along with Their NMR Predicted Puckering Percentage Preferences



Considering that the improvement of glycans' parameter set should maintain compatibility with the general GROMOS3A6 force field for other biomolecules, that is, proteins, nucleic acids, and lipids, the present work intends to expand the GROMOS 45A4/53A6 force field for carbohydrates. As the previous studies have shown, the limitation of such parameters resided in the adequate description of the preferred aldohexopyranose puckering conformations. To overcome this issue, the torsional energy profiles of model compounds representing the ring atoms were derived to describe their quantum-mechanical (QM) profiles. On the basis of these data, two novel potentials are proposed, which compose the new version of the herein modified GROMOS force field, referred to as GROMOS 53A6<sub>GLYC</sub>. Accordingly, such new parameters allow a proper description of the most stable conformation of hexopyranose-based monosaccharides, suitably enabling the study of saccharides either in solution or complexed to other

classes of biomolecules, in a landscape of structures resembling the existing biological complexity for aldohexopyranoses.

## METHODS

**Nomenclature and Software.** The nomenclature recommendations and symbols were used as proposed by IUPAC.<sup>33</sup> The QM calculations were performed with GAUSSIAN 98.<sup>34</sup> The equilibrium MD simulations were carried out with the standard version of GROMACS simulation suite version 4.5.1,<sup>35</sup> while metadynamics calculations<sup>36</sup> were performed using a modified version of GROMACS 4.5.1 interfaced with the PLUMED plugin package, version 1.2.2.<sup>37</sup> The free energy surfaces were obtained through the PLUMED package *sum\_hills* tool. The relative orientation of a contiguous pair of carbohydrate residues is described by two or three torsional angles at the glycosidic linkage. For a (1→X) linkage, where 'X'

is '3', '4', or '6' for the (1→3), (1→4), or (1→6) linkages, respectively, the  $\phi$  and  $\psi$  are defined as shown in eqs 1 and 2:

$$\phi = \text{O5} - \text{C1} - \text{OX} - \text{CX} \quad (1)$$

$$\psi = \text{C1} - \text{OX} - \text{CX} - \text{C(X-1)} \quad (2)$$

For a (1→6) linkage, the  $\omega$  is defined as shown below:

$$\omega = \text{O6} - \text{C6} - \text{C5} - \text{C4} \quad (3)$$

Comparatively, in unmodified monosaccharides, the  $\phi$ , employed for evaluating the hydroxymethyl group orientation, is defined as shown below:

$$\varpi = \text{O6} - \text{C6} - \text{C5} - \text{O5} \quad (4)$$

Finally, for a (1→1) linkage, the  $\phi$  and  $\phi'$  are defined as shown below:

$$\phi = \text{O5} - \text{C1} - \text{O1} - \text{C1}' \quad (5)$$

$$\phi' = \text{C1} - \text{O1} - \text{C1}' - \text{O5}' \quad (6)$$

**QM Calculations.** The QM torsional profiles for the rotations around C–C and C–O bonds, which comprise the dihedral angles determining pyranose ring conformations (C<sub>x</sub>–C<sub>x</sub>–C<sub>x</sub>–C<sub>x</sub>, C<sub>x</sub>–C<sub>x</sub>–O<sub>5</sub>–C<sub>x</sub>, and C<sub>x</sub>–C<sub>x</sub>–C<sub>x</sub>–O<sub>x</sub>) were determined, respectively, for the heavy atoms of model compounds CH<sub>3</sub>–CH<sub>2</sub>–CH<sub>2</sub>–CH<sub>3</sub>, CH<sub>3</sub>–CH<sub>2</sub>–O–CH<sub>3</sub>, and CH<sub>3</sub>–CH<sub>2</sub>–CH<sub>2</sub>–OH by increments of 30° at the HF/6-31G\* level of theory. This level of theory was chosen to ensure compatibility with the previously derived torsional parameters for the force field. However, it is worth noting that calculations at the MP2/6-31G\* and MP2/6-31G\*\* levels of theory were also carried out and showed a negligible difference in the relative energies for the different conformers as calculated with HF/6-31G\* (data not shown for conciseness). Each single-point calculation involved starting from the fully optimized conformation of each conformer, which were generated by rotating the selected dihedral angle to its target value, and then fully reoptimizing all other degrees of freedom. Subsequently, the same procedure was repeated at the molecular-mechanical level using fully optimized structures (conjugated-gradients) with a harmonic dihedral-angle restraining potential of 10 kJ mol<sup>−1</sup> deg<sup>−2</sup> force constant on each specific dihedral angle. The differences between QM and molecular-mechanical profiles were fitted by a cosine series, which served to determine whether changes in force field torsional parameters were required.

**Molecular Systems.** For metadynamics and unbiased MD simulations, 16 aldopyranoses were evaluated, comprised of D-allose (All), D-altrose (Alt), D-galactose (Gal), D-glucose (Glc), D-gulose (Gul), D-idose (Ido), D-mannose (Man), and D-talose (Tal) in both  $\alpha$  and  $\beta$  anomeric states (Chart 1). Additionally, eight disaccharides were also studied,  $\alpha$ -Glc–(1→1)-Glc (trehalose),  $\beta$ -Gal–(1→4)-Glc (lactose),  $\alpha$ -Glc–(1→4)-Glc (maltose),  $\beta$ -Glc–(1→4)-Glc (cellobiose),  $\alpha$ -Glc–(1→3)-Glc (nigerose),  $\beta$ -Glc–(1→3)-Glc (laminarabiose),  $\alpha$ -Gal–(1→6)-Glc (melibiose), and  $\beta$ -Glc–(1→6)-Glc (gentiobiose). The systems consisted of each carbohydrate centered in a triclinic box, with each axis presenting 3.6 nm, filled with ca. 1512 SPC water molecules.<sup>38</sup> Monosaccharides were assessed under three different conditions: (1) described by the current GROMOS 45A4/53A6 parameters,<sup>21</sup> (2) the new GROMOS 53A6<sub>GLYC</sub> parameter set, and (3) employing the GLYCAM06 force field parameters.<sup>14</sup> The disaccharide units were only evaluated under condition 2, by the new GROMOS 53A6<sub>GLYC</sub> parameter set to

assess their glycosidic linkage conformation in comparison to previous NMR data.<sup>39–45</sup>

**MD Simulation.** During all of the calculations, the Lincs method<sup>46</sup> was applied to constrain covalent bond lengths, allowing an integration step of 2 fs, while long-range electrostatic interactions were treated by the reaction field method<sup>47</sup> with  $\epsilon = 66$ . A 1.2 nm cutoff was used for the short-range electrostatics and van der Waals interactions. The temperature was maintained at 298 K by coupling solute and solvent separately with Nosé–Hoover thermostats<sup>48,49</sup> with a relaxation time of 0.1 ps. Pressure was kept at 1 bar using a Parrinello–Rahman barostat<sup>50,51</sup> via an isotropic coordinate scaling with a coupling constant of 1.0 ps and a compressibility of  $4.5 \times 10^{-5}$  bar<sup>−1</sup>. A 1 ns MD simulation was performed as an equilibration period and was not taken into account to calculate the average ensemble properties. Metadynamics calculations for the studied aldohexopyranoses consisted of 8 ns MD simulations, employing a height of 0.1 for the Gaussian height and a  $\sigma$  of 0.5 to each of the  $\theta$  and  $\phi$  angular coordinates of Cremer and Pople.<sup>52</sup> For the evaluated disaccharides, a 10 ns MD simulations was used, employing a height of 0.1 for the Gaussian height and a  $\sigma$  of 0.5 to each of the  $\phi$  and  $\psi$  glycosidic linkage dihedral angles. Also, 1  $\mu$ s MD simulations were performed employing unbiased MD simulations for all aldohexopyranoses and disaccharides studied.

## RESULTS AND DISCUSSION

**Force Field Parametrization.** The atomic charges for carbohydrate residues (Table 1), the potentials for bond stretching, bond-angle bending, and improper dihedral deformation (Table 2), as well as van der Waals interactions terms were retrieved directly from the GROMOS 45A4/53A6 functional form for carbohydrates,<sup>21,24</sup> previously validated elsewhere.<sup>21,53–55</sup>

The functional form of the potential-energy term, associated with the stretching of bond  $m$ , is given by

$$V_{b,m} = (1/4)k_{b,m}[b_m^2 - b_{o,m}^2]^2 \quad (7)$$

and it is applied to all unique pairs of covalently linked atoms that match those specified in Table 2, where  $b_m$  is the bond-length distance,  $b_o$  its reference value, and  $k_{b,m}$  the corresponding (quartic) force constant. The functional form of the potential-energy term, associated with the bending of bond angle  $m$ , is given by

$$V_{\theta,m} = (1/2)k_{\theta,m}[\cos \theta_m - \cos \theta_{o,m}]^2 \quad (8)$$

and it is applied to all unique triplets of covalently linked atoms that match those specified in Table 2, where  $\theta_m$  is the bond-angle value,  $\theta_o$  its reference value, and  $k_{\theta,m}$  the corresponding (cosine-harmonic) force constant. The functional form of the potential-energy term, associated with the deformation of improper-dihedral angle  $m$ , is given by

$$V_{\xi,m} = (1/2)k_{\xi,m}[\xi_m - \xi_{o,m}]^2 \quad (9)$$

and it is only applied, for each hexopyranose monomer, to the subset of improper-dihedral angles specified in Table 2, where  $\xi_m$  is the improper-dihedral angle value,  $\xi_o$  its reference value, and  $k_{\xi,m}$  the corresponding (harmonic) force constant. While some of the torsional potentials were preserved from the GROMOS 53A6 parameter set, those determining the conformation of the hexopyranose rings (C<sub>x</sub>–C<sub>x</sub>–C<sub>x</sub>–C<sub>x</sub>, C<sub>x</sub>–C<sub>x</sub>–O<sub>5</sub>–C<sub>x</sub>, and C<sub>x</sub>–C<sub>x</sub>–C<sub>x</sub>–O<sub>x</sub>) were re-evaluated

**Table 1.** Atom Types, Atomic Partial Charges and Charge-Group Definitions of the New GROMOS 53A6<sub>GLYC</sub> Force Field for Hexopyranose-Based Carbohydrates<sup>a,b</sup>

atom	charge group	atom type	partial atomic charge
4-OH initiation patch <sup>c</sup>			
O4	1	OA	−0.642
HO4	1	H	0.410
monomeric unit			
C4	1	CH <sub>1</sub>	0.232
C3	2	CH <sub>1</sub>	0.232
O3	2	OA	−0.642
HO3	2	H	0.410
C2	3	CH <sub>1</sub>	0.232
O2	3	OA	−0.642
HO2	3	H	0.410
C6	4	CH <sub>2</sub>	0.232
O6	4	OA	−0.642
HO6	4	H	0.410
C5	5	CH <sub>1</sub>	0.376
O5	5	OA	−0.480
1-OH termination patch <sup>d</sup>			
C1	5	CH <sub>1</sub>	0.232
O1	5	OA	−0.538
HO1	5	H	0.410
(1→X) glycosidic linkage (X corresponding to 2, 3, 4, or 6)			
C1	5	CH <sub>1</sub>	0.232
O1	5	OA	−0.360
Cx	5	CH <sub>1</sub>	0.232
1-OCH <sub>3</sub> termination patch <sup>d</sup>			
C1	5	CH <sub>1</sub>	0.232
O1	5	OA	−0.360
C <sub>Me</sub>	5	CH <sub>3</sub>	0.232

<sup>a</sup>The charge set is reported in the context of a (1→4)-linked hexopyranose unit, but the table is easily transferable to other linkages. An example for building a (1→1) termination patch may be found elsewhere in the literature.<sup>21</sup> <sup>b</sup>The rules for excluded atoms and third-neighbors follow the GROMOS conventions,<sup>53</sup> except for an additional exclusion between the ring oxygen O5 and the lactol hydrogen HO1 in residues terminated by a 1-OH patch. <sup>c</sup>A monosaccharide molecule or the first residue in an unbranched saccharide must be initiated by a 4-OH initiation patch, with the inclusion of the shown atoms. <sup>d</sup>A monosaccharide molecule or the last residue in an unbranched saccharide must be terminated by a 1-OH or a 1-OCH<sub>3</sub> termination patch.

based on fitting to QM data due to the so far reported difficulties of 53A6 parameters to reproduce ring puckering conformational properties. The functional form of the potential energy term, associated with the torsion around dihedral angle  $m$ , is given by

$$V_{\phi,m} = k_{\phi,m} [1 + \cos \delta_m \cos(n_m \phi_m)] \quad (10)$$

where  $\phi_m$  is the dihedral angle value,  $n_m$  the multiplicity of the term,  $\delta_m$  the associated phase shift, and  $k_{\phi,m}$  the corresponding force constant, which are applied, for each hexopyranose monomer, to a subset of dihedral angles as specified in Table 3.

It is worth noting that a given dihedral angle may be involved in more than one torsional potential energy term with different multiplicities and/or phase shifts. Accordingly, the classical energy profiles obtained from their rotation were compared to energy profiles obtained from QM calculations, as presented in Figure 1. From such analyses, torsional parameters for Cx–Cx–Cx–Cx and Cx–Cx–O5–Cx dihedral angles, as presented in

**Table 2.** Bond Stretching, Bond-Angle Bending, and Improper-Dihedral Deformation Parameters Employed in GROMOS 53A6<sub>GLYC</sub> Force Field for Hexopyranose-Based Carbohydrates

bond type	$k_b$ [ $10^6$ kJ mol <sup>−1</sup> nm <sup>−4</sup> ] <sup>a</sup>	$b_o$ [nm]
C–C	5.43	0.152
C–O	6.10	0.144
C–H	15.70	0.100
bond-angle type	$k_\theta$ [kJ mol <sup>−1</sup> ] <sup>b</sup>	$\theta_o$ [deg]
C–C–C	285	109.5
C–C–O	320	109.5
O–C–O	320	109.5
C–O–C	380	109.5
C–O–H	450	109.5
improper dihedral (assuming a chair <sup>4</sup> C <sub>1</sub> puckering)	$k_\xi$ [kJ mol <sup>−1</sup> deg <sup>−2</sup> ] <sup>c</sup>	$\xi_o$ [deg]
C1–O1–O5–C2 ( $\beta$ -anomer)	0.102	35.2644
C1–O5–O1–C2 ( $\alpha$ -anomer)	0.102	35.2644
C2–O2–C3–C1 (equatorial 2-OH)	0.102	35.2644
C2–C3–O2–C1 (axial 2-OH)	0.102	35.2644
C3–O3–C2–C4 (equatorial 3-OH)	0.102	35.2644
C3–C2–O3–C4 (axial 3-OH)	0.102	35.2644
C4–C3–O4–C5 (equatorial 4-OH)	0.102	35.2644
C4–O4–C3–C5 (axial 4-OH)	0.102	35.2644
C5–O5–C6–C4 (equatorial 6-CH <sub>2</sub> OH)	0.102	35.2644
C5–C6–O5–C4 (axial 6-CH <sub>2</sub> OH)	0.102	35.2644

<sup>a</sup>The parameters refer to eq 7. <sup>b</sup>The parameters refer to eq 8. <sup>c</sup>The parameters refer to eq 9.

the GROMOS 45A4/53A6 force field, are nearly identical to that from QM gas phase calculations (Figure 1A,B). On the other hand, important divergences between QM-calculated and 45A4/53A6 energy profiles for the Cx–Cx–Cx–Ox dihedral are observed (Figure 1C). Although accounting for two minimum-energy geometries, at 60° and 300°, the conformational barriers obtained for the current classical parameters are not sufficiently elevated to properly describe the rotation of such a dihedral. Additionally, the 180° conformer is described as the energy global maximum, instead of a local minimum (Figure 1C). On the basis of these data, two new torsional dihedral potentials associated with the rotation of the C–C–C–O dihedral angle were obtained by fitting the corresponding classical energy profiles to energy profiles obtained from QM calculations (Figure 1C). The resulting potentials, (1) a constant force of 5.88 kJ mol<sup>−1</sup>, a phase shift of 0, and multiplicity 1 and (2) a constant force of 7.67 kJ mol<sup>−1</sup>, phase shift of 0, and multiplicity of 3, were shown to adequately reproducing the QM-obtained energy profile related to such torsion. Consequently, those potentials were introduced to the torsional parameter set list (Table 3) for the GROMOS 53A6<sub>GLYC</sub> force field.

**Hexopyranoses Puckering Evaluation through Pseudotorsional Free Energy.** Adaptive biasing or flat histogram methods have been successfully used to compare force field accuracy, including the study of sugar puckering profiles.<sup>31,56,57</sup> Similarly, here a series of metadynamics calculations<sup>36</sup> was performed in order to evaluate whether the new parameter set was capable of reproducing the conformational profile of aldohexopyranose-based carbohydrates. For comparison purposes, the current GROMOS 45A4/53A6 force field was evaluated. It shows the <sup>4</sup>C<sub>1</sub> chair form as the most stable configuration for the 16 aldohexopyranoses (Table 4,



**Table 3.** Torsional Dihedral Interaction Parameters Used in the GROMOS 53A6<sub>GLYC</sub> Force Field for Hexopyranose-Based Carbohydrates

dihedral angle	$k_{\phi}$ [kJ mol <sup>-1</sup> ] <sup>a</sup>	$\delta$	$n$
C1–C2–C3–C4	5.92	0	3
C2–C3–C4–C5	5.92	0	3
C3–C4–C5–C6	5.92	0	3
O4–C4–C3–O3	2.09	0	2
O3–C3–C2–O2	2.09	0	2
O2–C2–C1–O1	2.09	0	2
C2–C1–O5–C5	3.77	0	3
C1–O5–C5–C4	3.77	0	3
O1–C1–C2–C3	5.88	0	1
O1–C1–C2–C3	7.67	0	3
O2–C2–C3–C4	5.88	0	1
O2–C2–C3–C4	7.67	0	3
O3–C3–C2–C1	5.88	0	1
O3–C3–C2–C1	7.67	0	3
O3–C3–C4–C5	5.88	0	1
O3–C3–C4–C5	7.67	0	3
O4–C4–C3–C2	5.88	0	1
O4–C4–C3–C2	7.67	0	3
O4–C4–C5–C6	5.88	0	1
O4–C4–C5–C6	7.67	0	3
O5–C1–C2–C3	5.88	0	1
O5–C1–C2–C3	7.67	0	3
O5–C5–C4–C3	5.88	0	1
O5–C5–C4–C3	7.67	0	3
C1–C2–O2–HO2	3.90	0	3
C2–C3–O3–HO3	3.90	0	3
C3–C4–O4–HO4	3.90	0	3
C5–C6–O6–HO6	3.90	0	3
O5–C5–C6–O6 <sup>b</sup>	9.50	0	3
O5–C5–C6–O6 <sup>b</sup>	9.35	180	1
O5–C5–C6–O6 <sup>c</sup>	7.69	0	3
O5–C5–C6–O6 <sup>c</sup>	6.66	180	1
C4–C5–C6–O6 <sup>c</sup>	2.67	180	1
O5–C1–O1–HO1 ( $\alpha$ anomer)	3.65	0	3
O5–C1–O1–HO1 ( $\alpha$ anomer)	9.45	180	1
O5–C1–O1–Ox ( $\alpha$ anomer)	3.65	0	3
O5–C1–O1–Ox ( $\alpha$ anomer)	9.45	180	1
O5–C1–O1–HO1 ( $\beta$ anomer)	4.69	0	3
O5–C1–O1–HO1 ( $\beta$ anomer)	3.41	180	1
O5–C1–O1–Ox ( $\beta$ anomer)	4.69	0	3
O5–C1–O1–Ox ( $\beta$ anomer)	3.41	180	1

<sup>a</sup>The parameters refer to eq 10. <sup>b</sup>Term to be used when the O4 and C6 atoms are on opposite sides of the ring plane (that is, equatorial–equatorial or axial–axial, as in glucose). <sup>c</sup>Term to be used when the O4 and C6 atoms are on the same side of the ring plane (that is, equatorial–axial or axial–equatorial, as in galactose).

first column). Proper description of ring pucker was obtained for all but one monosaccharide ( $\alpha$ -Ido) using the GROMOS 45A4/53A6 force field. It is worth noting that Autieri and co-workers have reported the inability of this parameter set to properly describe the ring pucker of two monosaccharides,  $\alpha$ -Ido and  $\beta$ -Tal.<sup>31,32</sup> Such discrepancy is likely due to the different simulation setups. Besides adoption of different values of  $\sigma$  and height, the present metadynamics simulations were carried out over an 8 ns period, in comparison with the previously published 4 ns time interval.<sup>31</sup> In contrast, the GROMOS 53A6<sub>GLYC</sub> has properly described the conforma-

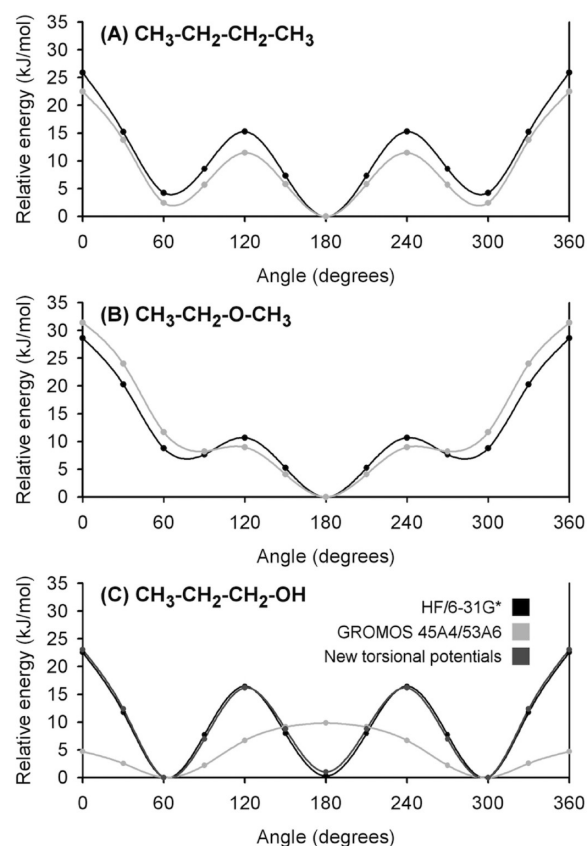


**Figure 1.** Comparison of energy profiles calculated at classical (45A4/53A6) and QM (HF/6-31G\*) levels in the gas phase. In A–C, the energy profiles for the rotation of the heavy atoms composing the model compounds CH<sub>3</sub>–CH<sub>2</sub>–CH<sub>2</sub>–CH<sub>3</sub>, CH<sub>3</sub>–CH<sub>2</sub>–O–CH<sub>3</sub>, and CH<sub>3</sub>–CH<sub>2</sub>–CH<sub>2</sub>–OH dihedral angles are respectively presented, as obtained from QM (black), the current torsional potentials (light gray), and the novel, derived torsional potentials (dark gray).

tional preferences of all evaluated monosaccharides, that is, the <sup>1</sup>C<sub>4</sub> conformation as the most stable ring puckering form for  $\alpha$ -Ido and <sup>4</sup>C<sub>1</sub> as the preferred state for the remaining aldohexopyranoses (Table 4, second column). In addition, a broader comparison with the GROMOS 53A6<sub>GLYC</sub> force field was also carried out by obtaining topology and coordinate files for GLYCAM06 from the GLYCAM Web site<sup>14</sup> and by converting them into GROMACS readable files with the *acpype* code.<sup>58</sup> Corresponding metadynamics simulations were carried out and the puckering free energies calculated. The latter differed from those performed with GROMOS 53A6<sub>GLYC</sub> only by the use of the TIP3P water model,<sup>59</sup> instead of SPC.<sup>38</sup> Our results show that GLYCAM06 parameters did not successfully describe the ring puckering preferential configurations for the  $\alpha$ -anomers of three monosaccharides, All, Alt, and Gul (Table 4, third column). A common point is that they present an axial C-3 linked hydroxyl group. Although Ido is not available for study in the GLYCAM Web site,<sup>14</sup> a previous publication involving an Ido-derived monosaccharide,  $\alpha$ -L-iduronic acid, also suggested that the GROMOS96 parameter set can better predict ring puckering conformational transitions in comparison to experimental data than GLYCAM06.<sup>60</sup> Altogether, based on the performed metadynamics calculations, the GROMOS 53A6<sub>GLYC</sub> force field was observed as capable of qualitatively reproducing the most stable ring puckering conformation of the 16 aldohexopyranose-based monosacchar-

**Table 4.** Difference between of Relative Free Energies ( $\text{kJ mol}^{-1}$ ) of  ${}^4\text{C}_1$  and  ${}^1\text{C}_4$  Puckering Conformations Associated with the Simulated Hexopyranoses, in Comparison with Chair Conformer Populations Obtained from NMR Experimental Data<sup>a</sup>

aldohexopyranose		GROMOS 53A6	GROMOS 53A6 <sub>GLYC</sub>	GLYCAM06	NMR ${}^4\text{C}_1/{}^1\text{C}_4$ (%/%)
All	$\alpha$	−26	−14	+31	100:0
	$\beta$	−31	−46	−4	100:0
Alt	$\alpha$	−28	−5	+25	66:34
	$\beta$	−21	−28	−7	90:10
Gal	$\alpha$	−10	−40	−18	100:0
	$\beta$	−18	−54	−38	100:0
Glc	$\alpha$	−18	−49	−11	100:0
	$\beta$	−31	−77	−41	100:0
Gul	$\alpha$	−28	−6	+25	100:0
	$\beta$	−30	−20	−15	100:0
Ido	$\alpha$	−26	+20	<sup>b</sup>	20:80
	$\beta$	−25	−13	<sup>b</sup>	75:25
Man	$\alpha$	−11	−23	−6	100:0
	$\beta$	−11	−59	−31	100:0
Tal	$\alpha$	−20	−2	−7	100:0
	$\beta$	−22	−40	−35	100:0

<sup>a</sup>The difference between the  ${}^4\text{C}_1$  and  ${}^1\text{C}_4$  chair conformations' relative free energy values are bolded when the most stable form of the aldohexopyranose monosaccharide is not properly described. <sup>b</sup>For GLYCAM06, the topology and coordinate files for  $\alpha$ - and  $\beta$ -Ido were not available for download in the Web site "Carbohydrate 3D Structure Predictor" section.

ides evaluated, with better results when compared to the current GROMOS 45A4/53A6 and GLYCAM06 force fields.

**Hexopyranoses Puckering Evaluation through Unrestrained MD.** In order to reinforce the results obtained with the metadynamics approach, each studied monosaccharide was further evaluated during a 1  $\mu\text{s}$  unrestrained MD simulation, described as the three parameter sets shown in Table 4, starting from each respective most stable conformation in solution ( ${}^1\text{C}_4$  for  $\alpha$ -Ido and  ${}^4\text{C}_1$  for the remaining aldohexopyranoses). From these data, as shown in Figure 2, it may be observed that, for the new GROMOS 53A6<sub>GLYC</sub> force field, each monosaccharide remained in their expected ring puckering conformation, and no transitions between minor conformational states could be observed. However, from the cited NMR data, there should be a 2:1 ratio of  ${}^4\text{C}_1$  to  ${}^1\text{C}_4$  conformers. From the NMR distributions, one could estimate the  ${}^4\text{C}_1 \rightarrow {}^1\text{C}_4$  conversion free energies (at 298.15 K) for  $\alpha$ -Alt (66:34),  $\beta$ -Alt (90:10),  $\alpha$ -Ido (20:80), and  $\beta$ -Ido (75:25) to be 1.7  $\text{kJ mol}^{-1}$ , 22.5  $\text{kJ mol}^{-1}$ , −3.5  $\text{kJ mol}^{-1}$ , and 2.7  $\text{kJ mol}^{-1}$ , respectively. The obtained values for  $\alpha$ -Alt (5  $\text{kJ mol}^{-1}$ ) and  $\beta$ -Alt (28  $\text{kJ mol}^{-1}$ ) are near quantitative to the estimated free energies, while the most probable conformations for  $\alpha$ -Ido and  $\beta$ -Ido seem over-stabilized. These results suggest the possibility of an intrinsic overall stabilization of the most probable puckering conformation of  $\beta$ -aldohexopyranoses. Nevertheless, variations in NMR derived data are not uncommon, as it is shown in Table 5 for the preferred conformation of the hydroxymethyl group in  $\beta$ -aldohexopyranoses.

For the GROMOS 45A4/53A6 force field, in agreement with the metadynamics data,  $\alpha$ -Ido was observed to converge from  ${}^1\text{C}_4$  to a  ${}^4\text{C}_1$  conformation at the beginning of the simulation, and to remain in such ring puckering state for the rest of the trajectory. Additionally, the monosaccharides' conformational

behavior with the GLYCAM06 parameter set presented a more variable profile (Figure 2). In accordance with the metadynamics results,  $\alpha$ -All,  $\alpha$ -Alt, and  $\alpha$ -Gul converged to the  ${}^1\text{C}_4$  ring puckering form, and all the  $\beta$ -anomers remained during all trajectories in their  ${}^4\text{C}_1$  state. The conformational stability of the GROMOS parameters are in contrast with GLYCAM generated ensembles, which have also shown multiple conformational states in previous publications.<sup>60</sup>

**Hydroxymethyl Group Rotation.** In comparison to the parameters set previously published for GROMOS 45A4/53A6 force field,<sup>21</sup> a discrepancy in one torsional potential related to the  $\phi$  dihedral angle (O5–C5–C6–O6) is found in the force field distribution within the GROMACS package. For the monosaccharides presenting the O4 and C6 atoms on the same side of the ring plane (that is, Gal, Gul, Ido, and Tal), one of such dihedrals presents a reduced constant force of 4.97  $\text{kJ mol}^{-1}$ , instead of the proposed 6.66  $\text{kJ mol}^{-1}$ . In order to assess whether such modification would alter the conformational profile of the  $\phi$  dihedral angle, we have analyzed its variation during the performed 1  $\mu\text{s}$  MD simulations. It is verified that the use of the decreased constant force promotes the higher population on the *tg* rotamer in Gal. The increased constant force is required for a proper description of the  $\phi$  angle of this monosaccharide, *i.e.*, a dominance of the *gt* rotamer in both anomers of Gal (Table 5), as well as similar populations of *tg* and *gg* rotamers, as shown by NMR data.<sup>61,62</sup> On the basis of the MD obtained data, among the remaining monosaccharides presenting the O4 and C6 atoms on the same side of the ring plane,  $\alpha$ - and  $\beta$ -Tal are those showing the same proportions of rotamers of Gal (Table 5), while the  ${}^1\text{C}_4$  conformation of  $\alpha$ -Ido promoted an increased population on the *gt* rotamer, similarly to Gal, and a small population related to the *tg* rotamer. On the other hand, for both anomers of Gul and for  $\beta$ -Ido, the *gg* rotamer is dominant (Table 5). The data suggest that such a difference is a feature of axial O3-presenting monosaccharides (Gul and Ido), which must be experimentally confirmed. Moreover, as a robust sampling could be obtained for the dynamics related to such dihedral, we have also analyzed its conformational profile for the remaining monosaccharides, presenting the O4 and C6 atoms on opposite sides of the ring plane (All, Alt, Glc, and Man), although no torsional parameter related to  $\phi$  was changed in the here presented GROMOS 53A6<sub>GLYC</sub> force field with respect to the GROMOS 45A4/53A6 parameter set. The relative populations for the *gg* (−60°), *gt* (60°), and *tg* (180°) conformers, as reported in Table 5, reproduce the small population related to the *tg* rotamer, as well as *gg* and *gt* rotamers with similar populations in Glc and Man, as observed from NMR-derived data.<sup>61–66</sup> Moreover, both anomers of All and Alt presented the same conformational profile.

**Glycosidic Linkages Conformation.** In order to assess whether the herein presented GROMOS 53A6<sub>GLYC</sub> force field is capable of properly describing the conformation of glycosidic linkage, we have performed 1  $\mu\text{s}$  MD simulations in eight selected disaccharides presenting known glycosidic linkage conformations, as previously described by NMR methods.<sup>39–45</sup> As displayed in Figure 3, the simulations reproduced very well the glycosidic linkage conformations in all cases. Particularly, the employed force field was capable of properly reproducing the *exo*-anomeric effect, in which the  $\phi$  dihedral angle of  $\alpha$ -anomers (Figure 3A, C, E, and G) is more populated at positive geometries ( $\sim 60^\circ$ ), while the  $\beta$ -anomers (Figure 3B, D, F, and H) may adopt two staggered conformations, at approximately

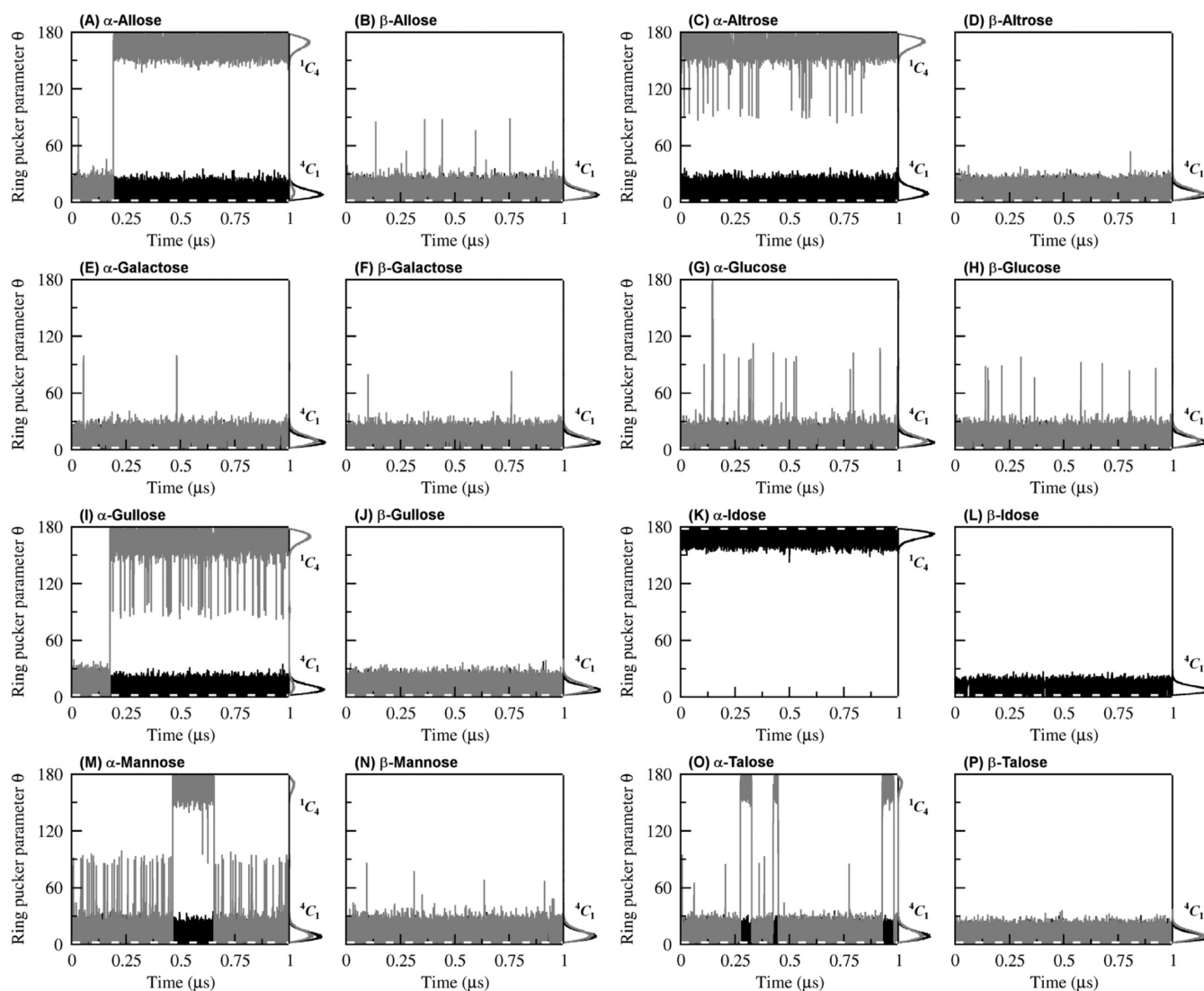


**Figure 2.** Fluctuations (curves) and distribution (side histograms) of the  $\theta$  ring pucker parameter during the 1  $\mu$ s MD simulations performed with the sixteen studied aldohexopyranoses, described as the new GROMOS 53A6<sub>GLYC</sub> (black) and GLYCAM06 (gray) force fields.  $\theta$  values close to 0 indicate a  ${}^4C_1$  conformation, while values close to 180 point to a  ${}^1C_4$  state. In the graphs, white dashed lines indicate the most populated ring pucker conformational state for each aldohexopyranose, as observed from experimental data.

$-60^\circ$  and  $60^\circ$ , but mostly negative values.<sup>67</sup> Regarding the  $\omega$  dihedral angle (O1–C6–C5–C4) of (1 $\rightarrow$ 6) linkages, only the three possible staggered conformations ( $-180^\circ$ ,  $-60^\circ$ , and  $60^\circ$ ) were populated, in accordance with Shefter and Trueblood's convention.<sup>68</sup> The GROMOS 53A6<sub>GLYC</sub> parameter set was also capable of adequately reproducing the *gauche* effect,<sup>69</sup> in which the  $-60^\circ$  conformation was mostly not observed in solution.

## CONCLUSIONS

In the current study, a new parameter set (GROMOS 53A6<sub>GLYC</sub>) was presented, in which we have proposed two new torsional potentials to be included within the previous GROMOS 45A4/53A6 force field for the simulation of hexopyranose-based carbohydrates. The major advantage over previously proposed modifications of the force field is that this approach is still compatible with the general GROMOS parameter set for other classes of biomolecules. The addition of new torsional potentials, instead of largely altering atom types and van der Waals nonbonded interactions, is a similar approach to that recently performed for improving GROMOS

parameters for proteins.<sup>70,71</sup> Moreover, the employment of a  $6.66 \text{ kJ mol}^{-1}$  force constant for a torsional potential parameter describing the  $\phi$  dihedral angle (O5–C5–C6–O6) of monosaccharides presenting the O4 and C6 atoms on the same side of the ring plane, as Gal, was confirmed necessary.

The new GROMOS 53A6<sub>GLYC</sub> force field is capable of properly describing the most stable ring pucker conformation of a set of 16 aldohexopyranoses, showing more accurate results than the GROMOS 45A4/53A6 and an ACPYPE-converted version of GLYCAM06. The new parameter set was also able to adequately reproduce the glycosidic linkage conformation of eight different disaccharides tested, as well as the relative abundance of the hydroxymethyl group in Gal, Glc, and Man anomers, both based on comparisons of previous solution NMR data with 1  $\mu$ s MD simulations achieved in the present study. Furthermore, as previously reported for the GROMOS 45A4/53A6 force field,<sup>21</sup> the GROMOS 53A6<sub>GLYC</sub> parameter set is suitable for MD simulation studies of any unbranched hexopyranose-based mono-, di-, oligo-, or polysaccharide. Nevertheless, as a continual upgrading is required to meet



**Table 5.** Relative Populations Associated with the Three Staggered Conformations of the Hydroxymethyl Group, As Obtained from 1  $\mu$ s MD Simulations for the 16 Studied Aldohexopyranoses

aldohexopyranose		$\phi^a$		
		$-60^\circ$ (gg)	$60^\circ$ (gt)	$180^\circ$ (tg)
All	$\alpha$	62	38	0
	$\beta$	60	40	0
Alt	$\alpha$	56	44	0
	$\beta$	53	47	0
Gal	$\alpha$	34 ( $21^b$ , $3^d$ ) [ $24^e$ ]	43 ( $54^b$ , $74^d$ ) [ $30^e$ ]	23 ( $25^b$ , $23^d$ ) [ $46^e$ ]
	$\beta$	32 ( $22^b$ , $3^d$ ) [ $21^e$ ]	42 ( $53^b$ , $72^d$ ) [ $30^e$ ]	26 ( $25^b$ , $25^d$ ) [ $49^e$ ]
Glc	$\alpha$	60 ( $56^b$ , $47^c$ , $40^d$ )	40 ( $44^b$ , $54^c$ , $53^d$ )	0 ( $0^b$ , $-1^c$ , $7^d$ )
	$\beta$	55 ( $53^b$ , $45^c$ , $31^d$ )	45 ( $45^b$ , $62^c$ , $61^d$ )	0 ( $2^b$ , $-7^c$ , $8^d$ )
Gul	$\alpha$	48 [ $36^e$ ]	33 [ $25^e$ ]	19 [ $39^e$ ]
	$\beta$	45 [ $33^e$ ]	34 [ $26^e$ ]	21 [ $41^e$ ]
Ido	$\alpha$	16 [ $15^e$ ]	80 [ $75^e$ ]	4 [ $10^e$ ]
	$\beta$	43 [ $31^e$ ]	37 [ $30^e$ ]	20 [ $39^e$ ]
Man	$\alpha$	53	47	0
	$\beta$	49 ( $48^e$ )	51 ( $49^e$ )	0 ( $3^e$ )
Tal	$\alpha$	38 [ $27^e$ ]	41 [ $31^e$ ]	21 [ $42^e$ ]
	$\beta$	35 [ $24^e$ ]	42 [ $30^e$ ]	23 [ $46^e$ ]

<sup>a</sup>The two letters in the notations *gt*, *tg*, and *gg* refer successively to the relative orientations of O6 relative to O5 (first letter, gauche or trans) and C4 (second letter, gauche or trans). The values between parentheses for Glc, Gal, and Man anomers correspond to relative populations derived from NMR experiments by <sup>b</sup>Nishida et al.<sup>61,63,64</sup> <sup>c</sup>Brochier-Salon and Morin.<sup>65</sup> <sup>d</sup>Thibaudeau et al.<sup>62</sup> <sup>e</sup>Hori et al.<sup>66</sup> Rotamer population using a force constant of 4.97 kJ mol<sup>-1</sup>.

the demands of the scientific community, we are looking forward to further refinement of the parameter set, as well as its

extension for a broader set of carbohydrates, such as acetylated sugar derivatives and furanoses.

## AUTHOR INFORMATION

### Corresponding Author

\*E-mail: roberto.lins@ufpe.br.

### Notes

The authors declare no competing financial interest.

## ACKNOWLEDGMENTS

This research was funded by CNPq, NanoBiotec-BR/CAPES, INCT-INAMI, FACEPE, nBioNet, and the Swedish Foundation for International Cooperation in Research and Higher Education (STINT). Part of the computational resources were provided by the Environmental Molecular Sciences Laboratory, a U.S. national scientific user facility sponsored by the U.S. Department of Energy located at the Pacific Northwest National Laboratory.

## REFERENCES

- (1) Turnbull, J. E.; Field, R. A. Emerging glycomics technologies. *Nat. Chem. Biol.* **2007**, *3*, 74–77.
- (2) Varki, A. Biological roles of oligosaccharides: all of the theories are correct. *Glycobiology* **1993**, *3*, 97–130.
- (3) Dwek, R. A. Glycobiology: toward understanding the function of sugars. *Chem. Rev.* **1996**, *96*, 683–720.
- (4) Lowe, J. B.; Marth, J. D. A genetic approach to mammalian glycan function. *Annu. Rev. Biochem.* **2003**, *72*, 643–691.
- (5) Petrescu, A. J.; Wormald, M. R.; Dwek, R. A. Structural aspects of glycomes with a focus on N-glycosylation and glycoprotein folding. *Curr. Opin. Struct. Biol.* **2006**, *16*, 600–607.
- (6) Woods, R. J. Computational carbohydrate chemistry: what theoretical methods can tell us. *Glycoconjugate J.* **1998**, *15*, 209–216.

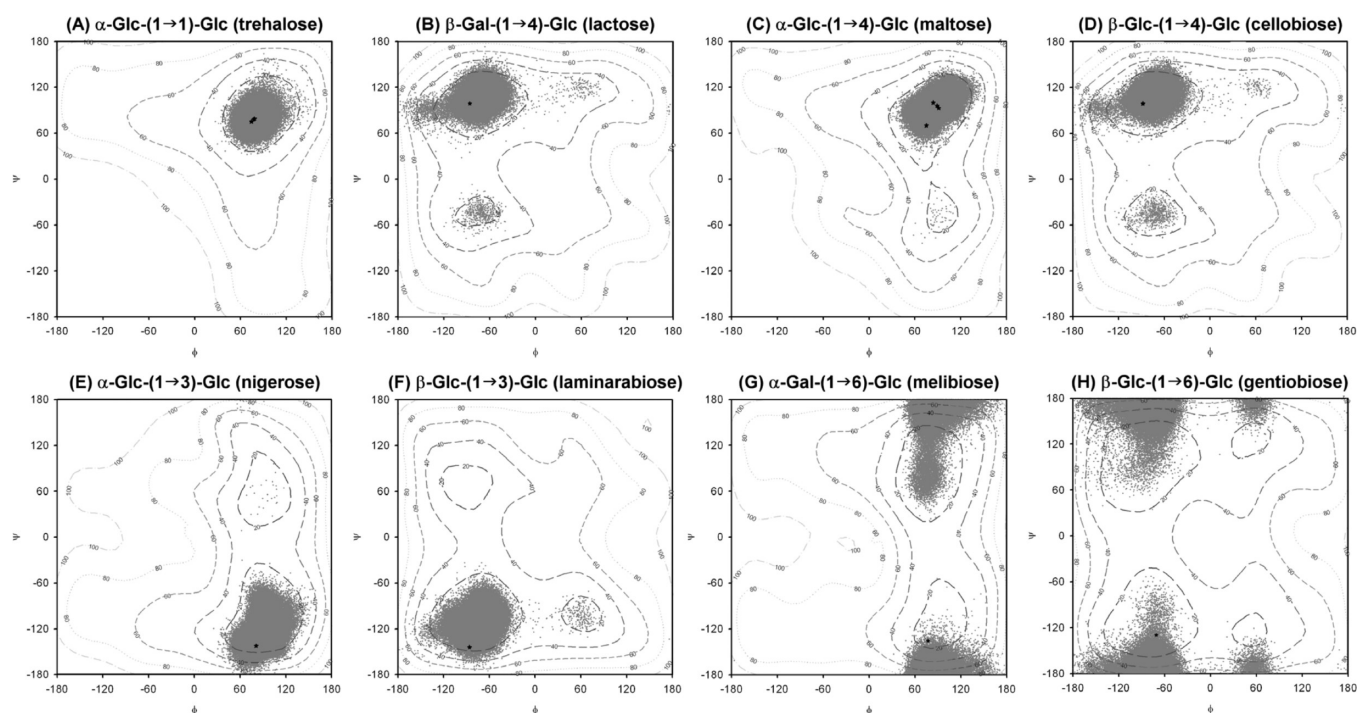


**Figure 3.** Contour plots for the glycosidic linkages of eight disaccharides, as obtained from metadynamics calculations. Free energy maps are shown at every 20 kJ mol<sup>-1</sup>, from 20 to 100 kJ mol<sup>-1</sup>. The corresponding solution profiles for the disaccharides from 1  $\mu$ s MD simulations are presented as gray dots at every 10 ps interval. Black dots indicate experimental glycosidic linkage geometries obtained from NMR.<sup>39–45</sup>



- (7) Mulloy, B.; Forster, M. J.; Jones, C.; Davies, D. B. N.M.R. and molecular-modelling studies of the solution conformation of heparin. *Biochem. J.* **1993**, 293, 849–858.
- (8) Bub, W. NMR spectroscopy in the study of carbohydrates: Characterizing the structural complexity. *Concepts Magn. Reson., Part A* **2003**, 19A, 1–13.
- (9) Blanchard, V.; Chevalier, F.; Imbert, A.; Leeftang, B. R.; Basappa, Sugahara, K.; Kamerling, J. P. Conformational studies on five octasaccharides isolated from chondroitin sulfate using NMR spectroscopy and molecular modeling. *Biochemistry* **2007**, 46, 1167–1175.
- (10) Pérez, S.; Kouwijzer, M. In *Carbohydrates: Structures, Dynamics and Syntheses*; Finch, P., Ed.; Kluwer Academic Press: Dordrecht, The Netherlands, 1999; pp 258–293.
- (11) Imbert, A.; Pérez, S. Structure, Conformation, and Dynamics of Bioactive Oligosaccharides: Theoretical Approaches and Experimental Validations. *Chem. Rev.* **2000**, 100, 4567–4588.
- (12) Hansen, H. S.; Hünenberger, P. H. A Reoptimized GROMOS Force Field for hexopyranose-Based Carbohydrates Accounting for the Relative Free Energies of Ring Conformers, Anomers, Epimers, Hydroxymethyl Rotamers, and Glycosidic Linkage Conformers. *J. Comput. Chem.* **2011**, 32, 998–1032.
- (13) Woods, R. J.; Dwek, R. A.; Edge, C. J.; Fraser-Reid, B. Molecular Mechanical and Molecular Dynamical Simulations of Glycoproteins and Oligosaccharides. 1. GLYCAM-93 Parameter Development. *J. Phys. Chem.* **1995**, 99, 3832–3846.
- (14) Kirschner, K. N.; Yongye, A. B.; Tschampel, S. M.; González-Outeiriño, J.; Daniels, C. R.; Foley, B. L.; Woods, R. J. GLYCAM06: A generalizable biomolecular force field. *Carbohydrates. J. Comput. Chem.* **2008**, 29, 622–655.
- (15) Kuttel, M.; Brady, J. W.; Naidoo, K. J. Carbohydrate solution simulations: Producing a force field with experimentally consistent primary alcohol rotational frequencies and populations. *J. Comput. Chem.* **2002**, 23, 1236–1243.
- (16) Guvench, O.; Greene, S. N.; Kamath, G.; Brady, J. W.; Venable, R. M.; Pastor, R. W.; Mackerell, A. D. J. Additive empirical force field for hexopyranose monosaccharides. *J. Comput. Chem.* **2008**, 29, 2543–2564.
- (17) Guvench, O.; Hatcher, E. R.; Venable, R. M.; Pastor, R. W.; Mackerell, A. D. J. CHARMM Additive All-Atom Force Field for Glycosidic Linkages between Hexopyranoses. *J. Chem. Theory Comput.* **2009**, 9, 2353–2370.
- (18) Raman, E. P.; Guvench, O.; Mackerell, A. D. J. CHARMM Additive All-Atom Force Field for Glycosidic Linkages in Carbohydrates Involving Furanoses. *J. Phys. Chem. B* **2010**, 114, 12981–12994.
- (19) Damm, W.; Frontera, A.; Tirado-Rives, J.; Jorgensen, W. OPLS all-atom force field for carbohydrates. *J. Comput. Chem.* **1997**, 18, 1955–1970.
- (20) Kony, D.; Damm, W.; Stoll, S.; van Gunsteren, W. F. An improved OPLS-AA force field for carbohydrates. *J. Comput. Chem.* **2002**, 23, 1416–1429.
- (21) Lins, R. D.; Hünenberger, P. H. New GROMOS Force Field for Hexopyranose-Based Carbohydrates. *J. Comput. Chem.* **2005**, 26, 1400–1412.
- (22) Verli, H.; Guimarães, J. A. Molecular dynamics simulation of a decasaccharide fragment of heparin in aqueous solution. *Carbohydr. Res.* **2004**, 339, 281–290.
- (23) Pol-Fachin, L.; Fernandes, C. L.; Verli, H. GROMOS96 43a1 performance on the characterization of glycoprotein conformational ensembles through molecular dynamics simulations. *Carbohydr. Res.* **2009**, 344, 491–500.
- (24) Oostenbrink, C.; Villa, A.; Mark, A. E.; van Gunsteren, W. F. A biomolecular force field based on the free enthalpy of hydration and solvation: the GROMOS force-field parameter sets 53A5 and 53A6. *J. Comput. Chem.* **2004**, 25, 1656–1676.
- (25) Pereira, C. S.; Kony, D.; Baron, R.; Müller, M.; van Gunsteren, W. F.; Hünenberger, P. H. Conformational and Dynamical Properties of Disaccharides in Water: a Molecular Dynamics Study. *Biophys. J.* **2006**, 90, 4337–4344.
- (26) Franca, E. F.; Lins, R. D.; Freitas, L. C. G.; Straatsma, T. P. Characterization of Chitin and Chitosan Molecular Structure in Aqueous Solution. *J. Chem. Theory Comput.* **2008**, 4, 2141–2149.
- (27) Horta, B. A. C.; Peric-Hassler, L.; Hünenberger, P. H. Interaction of the disaccharides trehalose and gentiobiose with lipid bilayers: A comparative molecular dynamics study. *J. Mol. Graphics Modell.* **2010**, 29, 331–346.
- (28) Horta, B. A. C.; Peric-Hassler, L.; Hünenberger, P. H. Interaction of the disaccharides trehalose and gentiobiose with lipid bilayers: A comparative molecular dynamics study. *J. Mol. Graphics Modell.* **2010**, 29, 331–346.
- (29) Franca, E. F.; Freitas, L. C. G.; Lins, R. D. Chitosan Molecular Structure as a Function of N-Acetylation. *Biopolymers* **2011**, 95, 448–460.
- (30) Fedorov, M. V.; Goodman, J. M.; Neruck, D.; Schumm, S. Self-assembly of trehalose molecules on a lysozyme surface: the broken glass hypothesis. *Phys. Chem. Chem. Phys.* **2011**, 13, 2294–2299.
- (31) Autieri, E.; Sega, M.; Pederiva, F.; Guella, G. Puckering free energy of pyranoses: a NMR and metadynamics-umbrella sampling investigation. *J. Chem. Phys.* **2010**, 133, 095104.
- (32) Autieri, E.; Sega, M.; Pederiva, F.; Guella, G. Erratum: “Puckering free energy of pyranoses: a NMR and metadynamics-umbrella sampling investigation” [*J. Chem. Phys.* 133, 095104 (2010)]. *J. Chem. Phys.* **2011**, 134.
- (33) McNaught, A. D. International Union of Pure and Applied Chemistry and International Union of Biochemistry and Molecular Biology - Joint Commission on Biochemical Nomenclature - Nomenclature of carbohydrates - Recommendations 1996. *Pure Appl. Chem.* **1996**, 68 (10), 1919–2008.
- (34) Frisch, M. J.; Trucks, G. W.; Schlegel, H. B.; Scuseria, G. E.; Robb, M. A.; Cheeseman, J. R.; Zakrzewski, V. G.; Stratmann, R. E.; Burant, J. C.; Dapprich, S.; Millam, J. M.; Daniels, A. D.; Kudin, K. N.; Strain, M. C.; Farkas, O.; Tomasi, J.; Barone, V.; Cossi, M.; Cammi, R.; Mennucci, B.; Pomelli, C.; Adamo, C.; Clifford, S.; Ochterski, J.; Petersson, G. A.; Ayala, P. Y.; Cui, Q.; Morokuma, K.; Rega, N.; Salvador, P.; Dannenberg, J. J.; Malick, D. K.; Rabuck, A. D.; Raghavachari, K.; Foresman, J. B.; Cioslowski, J.; Ortiz, J. V.; Baboul, A. G.; Stefanov, B. B.; Liu, G.; Liashenko, A.; Piskorz, P.; Komaromi, I.; Gomperts, R.; Martin, R. L.; Fox, D. J.; Keith, T.; Laham, A.; Peng, C. Y.; Nanayakkara, A.; Challacombe, M.; Gill, P. M. W.; Johnson, B.; Chen, W.; Wong, M. W.; Andres, J. L.; Gonzalez, C.; Gordon, H.; Replogle, E. S.; Pople, J. A. *Gaussian 98*, Revision A.11.4.; Gaussian, Inc.: Pittsburgh, PA, 2002.
- (35) Hess, B.; Kutzner, C.; van der Spoel, D.; Lindahl, E. GROMACS 4: Algorithms for highly efficient, load-balanced, and scalable molecular simulation. *J. Chem. Theory Comput.* **2009**, 4, 435–447.
- (36) Barducci, A.; Bonomi, M.; Parrinello, M. Metadynamics. *WIREs Comput. Mol. Sci.* **2011**, 1, 826–843.
- (37) Bonomi, M.; Branduardi, D.; Bussi, G.; Camilloni, C.; Provasi, D.; Raiteri, P.; Donadio, D.; Marinelli, F.; Pietrucci, F.; Broglia, R. A.; Parrinello, M. PLUMED: a portable plugin for free energy calculations with molecular dynamics. *Comput. Phys. Commun.* **2009**, 180, 1961–1972.
- (38) Berendsen, H. J. C.; Grigera, J. R.; Straatsma, T. P. The missing term in effective pair potentials. *J. Phys. Chem.* **1987**, 91, 6269–6271.
- (39) Cheetham, N. W. H.; Dasgupta, P.; Ball, G. E. NMR and modelling studies of disaccharide conformation. *Carbohydr. Res.* **2003**, 338, 955–962.
- (40) Parfondy, A.; Cyr, N.; Perlin, A. S. <sup>13</sup>C-<sup>1</sup>H inter-residue, coupling in disaccharides, and the orientations of glycosidic bonds. *Carbohydr. Res.* **1977**, 59, 299–309.
- (41) Shashkov, A. S.; Lipkind, G. M.; Kochetkov, N. K. Nuclear overhauser effects for methyl  $\beta$ -maltoside and the conformational states of maltose in aqueous solution. *Carbohydr. Res.* **1986**, 147, 175–182.
- (42) Pérez, S.; Taravel, F.; Vergelati, C. Experimental evidences of solvent induced conformational changes in maltose. *Nouv. J. Chim.* **1985**, 4, 561–564.

- (43) Poveda, A.; Vicent, C.; Penades, S.; Jimenez-Barbero, J. NMR experiments for the detection of NOEs and scalar coupling constants between equivalent protons in trehalose-containing molecules. *Carbohydr. Res.* **1997**, *301*, 5–10.
- (44) Batta, G.; Kover, K. E.; Gervay, J.; Hornyak, M.; Roberts, G. M. Temperature dependence of molecular conformation, dynamics, and chemical shift anisotropy of  $\alpha,\alpha$ -trehalose in D<sub>2</sub>O by NMR relaxation. *J. Am. Chem. Soc.* **1997**, *119*, 1336–1345.
- (45) Hayes, M. L.; Serianni, A. S.; Barker, R. Methyl  $\beta$ -lactoside: 600-MHz <sup>1</sup>H- and 75-MHz <sup>13</sup>C-n.m.r. studies of 2H- and <sup>13</sup>C-enriched compounds. *Carbohydr. Res.* **1982**, *100*, 87–100.
- (46) Hess, B.; Bekker, H.; Berendsen, H. J. C.; Fraaije, J. G. E. M. LINCS: a linear constraint solver for molecular simulations. *J. Comput. Chem.* **1997**, *18*, 1463–1472.
- (47) Tironi, I. G.; Sperb, R.; Smith, P. E.; van Gunsteren, W. F. A generalized reaction field method for molecular dynamics simulations. *J. Chem. Phys.* **1995**, *102*, 5451–5459.
- (48) Nosé, S. A molecular dynamics method for simulations in the canonical ensemble. *Mol. Phys.* **1984**, *52*, 255–268.
- (49) Hoover, W. G. Canonical dynamics: equilibrium phase-space distributions. *Phys. Rev. A* **1985**, *31*, 1695–1697.
- (50) Parrinello, M.; Rahman, A. Polymorphic transitions in single crystals: A new molecular dynamics method. *J. Appl. Phys.* **1981**, *52*, 7182–7190.
- (51) Nosé, S.; Klein, M. L. Constant pressure molecular dynamics for molecular systems. *Mol. Phys.* **1983**, *50*, 1055–1076.
- (52) Cremer, D.; Pople, J. A. A General Definition of Ring Puckering Coordinates. *J. Am. Chem. Soc.* **1975**, *97*, 1354–1358.
- (53) Scott, W. R. P.; Hünenberger, P. H.; Tironi, I. G.; Mark, A. E.; Billeter, S. R.; Fennen, J.; Torda, A. E.; Huber, T.; Krueger, P.; van Gunsteren, W. F. The GROMOS biomolecular simulation program. *J. Phys. Chem. A* **1999**, *103*, 3596–3607.
- (54) Schuler, L. D.; van Gunsteren, W. F. On the Choice of Dihedral Angle Potential Energy Functions for *n*-Alkanes. *Mol. Simul.* **2000**, *25*, 301–319.
- (55) Schuler, L. D.; Daura, X.; van Gunsteren, W. F. An Improved GROMOS96 Force Field for Aliphatic Hydrocarbons in the Condensed Phase. *J. Comput. Chem.* **2001**, *22*, 1205–1218.
- (56) Spiwok, V.; Králová, B.; Tvaroska, I. Modelling of  $\beta$ -D-glucopyranose ring distortion in different force fields: a metadynamics study. *Carbohydr. Res.* **2010**, *345*, 530–537.
- (57) Barnett, C. B.; Naidoo, K. J. Ring Puckering: A Metric for Evaluating the Accuracy of AM1, PM3, PM3CARB-1, and SCC-DFTB Carbohydrate QM/MM Simulations. *J. Phys. Chem. B* **2010**, *114*, 17142–17154.
- (58) Sousa da Silva, A. W.; Vranken, W. F.; Laue, E. D. ACPYPE – AnteChamber PYthon Parser interfAcE. Manuscript to be submitted.
- (59) Jorgensen, W. L.; Chandrasekhar, J.; Madura, J. D.; Impey, R. W.; Klein, M. L. Comparison of simple potential functions for simulating liquid water. *J. Chem. Phys.* **1983**, *79*, 926–935.
- (60) Gandhi, N. S.; Mancera, R. L. Can current force fields reproduce ring puckering in 2-O-sulfo- $\alpha$ -L-iduronic acid? A molecular dynamics simulation study. *Carbohydr. Res.* **2010**, *345*, 689–695.
- (61) Nishida, Y.; Ohnui, H.; Meguro, H. <sup>1</sup>H-NMR Studies of (6R)- and (6S)-Deuterated D-Hexoses: Assignment of the Preferred Rotamers about C5-C6 Bond of D-Glucose and D-Galactose Derivatives in Solutions. *Tetrahedron Lett.* **1984**, *25*, 1575–1578.
- (62) Thibault, C.; Stenutz, R.; Hertz, B.; Klepach, T.; Zhao, S.; Wu, Q.; Carmichael, I.; Serianni, A. S. Correlated C-C and C-O bond conformations in saccharide hydroxymethyl groups: parametrization and application of redundant <sup>1</sup>H-<sup>1</sup>H, <sup>13</sup>C-<sup>1</sup>H, and <sup>13</sup>C-<sup>13</sup>C NMR J-couplings. *J. Am. Chem. Soc.* **2004**, *126*, 15668–15685.
- (63) Ohnui, H.; Nishida, Y.; Higuchi, H.; Hori, H.; Meguro, H. The preferred rotamer about the C5-C6 bond of D-galactopyranoses and the stereochemistry of dehydrogenation by D-galactose oxidase. *Can. J. Chem.* **1987**, *65*, 1145–1153.
- (64) Nishida, Y.; Hori, H.; Ohnui, H.; Meguro, H. <sup>1</sup>H NMR Analyses of Rotameric Distribution of C5-C6 bonds of D-Glucopyranoses in Solution. *J. Carbohydr. Chem.* **1988**, *7*, 239–250.
- (65) Brochier-Salon, M.-C.; Morin, C. Conformational analysis of 6-deoxy-6-iodo-D-glucose in aqueous solution. *Magn. Reson. Chem.* **2000**, *38*, 1041–1042.
- (66) Hori, H.; Nishida, Y.; Ohnui, H.; Meguro, H. Conformational Analysis of Hydroxymethyl Group of D-Mannose Derivatives Using (6S)- and (6R)-(6-<sup>2</sup>H1)-D-Mannose. *J. Carbohydr. Chem.* **1990**, *9*, 601–618.
- (67) Rao, V. S. R.; Qasba, P. K.; Balaji, P. V.; Chandrasekaran, R. Conformation of Disaccharides. In *Conformation of Carbohydrates*; Rao, V. S. R., Ed.; Harwood Academic: The Netherlands, 1998; pp 91–130.
- (68) Shefter, E.; Trueblood, K. N. The crystal and molecular structure of D(+)-barium uridine-5'-phosphate. *Acta Crystallogr.* **1965**, *18*, 1067–1077.
- (69) Wolfe, S. Gauche effect. Stereochemical consequences of adjacent electron pairs and polar bonds. *Acc. Chem. Res.* **1972**, *5*, 102–111.
- (70) Schmid, N.; Eichenberger, A.; Choutko, A.; Riniker, S.; Winger, M.; Mark, A. E.; van Gunsteren, W. F. Definition and testing of the GROMOS force-field versions 54A7 and 54B7. *Eur. Biophys. J.* **2011**, *40*, 843–856.
- (71) Huang, W.; Lin, Z.; van Gunsteren, W. F. Validation of the GROMOS 54A7 Force Field with Respect to  $\beta$ -Peptide Folding. *J. Chem. Theory Comput.* **2011**, *7*, 1237–1243.